

Understanding the Bonding Mechanisms of Directly Sputtered Copper Thin Film on an Alumina Substrate

Ju Dy Lim^{a,b}, Pui Mun Lee^c, Zhong Chen^a

^a *School of Materials Science and Engineering, Nanyang Technological University, Singapore 639798*

^b *GLOBALFOUNDRIES Pte Ltd, Singapore 738406*

^c *Interdisciplinary Graduate School, Nanyang Technological University, Singapore 639798*

Abstract

The evaluation of bonding mechanisms between magnetron sputtered copper (Cu) thin films and a ceramic substrate was carried out using polycrystalline and monocrystalline alumina (Al₂O₃) substrates with different surface roughness. Three different bonding mechanisms, *viz.*, surface adsorption, mechanical interlocking, and diffusion bonding have been assessed. A tensile test was applied to measure the interfacial adhesion strength between the Cu films and the Al₂O₃ substrate. The contribution to the interfacial adhesion from each of the bonding mechanisms was elucidated based on the adhesion strength. Without special surface pre-treatment, physical adsorption is the main factor for the film adhesion, contributing ~5.9 MPa adhesion strength between this directly sputtered Cu film and a flat Al₂O₃ substrate. For substrates with surface roughness around 350 - 500 nm, mechanical interlocking enhances the film adhesion up to 18.6 % compared to the flat surface. Post-deposition annealing at 300 °C has increased adhesion strength by 18 %, and diffusion bonding may be operative.

Keywords: Copper-Alumina Bonding; Surface Roughness; Adhesion Strength; Bonding Mechanism; Contact Area

Corresponding authors

jdlim3@e.ntu.edu.sg; aszchen@ntu.edu.sg

Nanyang Avenue, Singapore 639798

Tel: +65 96437005; +65 67904256

1. Introduction

The topic of adhesion has been well known in the scientific community due to its wide range of applications in microelectronics and other industries. Research on adhesion has been extensively carried out for improvement of the interfacial joining between materials. In microelectronic packaging, ceramic metallization is the subject of interest and has been extensively studied mechanically, chemically and electrically [1-6] due to its unique properties specifically under extreme environments. Although this topic has been extensively studied and various bonding techniques have been reported, many open questions are still left to be addressed in a systematic way to understand and improve the device reliability.

According to Zhang et al. [7], mechanical failure is the major failure path in microelectronic devices, and interfacial debonding between heterogeneous materials is a great concern for reliability. To enhance the adhesion, bonding parameters during processing have to be optimized. Different factors including surface pre-treatment, surface cleanliness, joining techniques, etc., are essential to be considered. For Cu-Al₂O₃ bonding, various bonding methods such as eutectic joining [8], transient liquid bonding [9], cold gas spraying [10] and casting bonding [5] have been studied to achieve optimized adhesion. However, these methods typically require a high processing temperature, and the process is not compatible with the existing packaging industry practice. For low temperature metallization, an adhesion layer (typically Ti/W) is often needed due to the poor wetting of Cu thin films to the ceramic substrate. Direct coating without the adhesion layer has a clear advantage, but the bonding mechanism between directly coated metal thin films and ceramic substrates is yet to be clarified, especially in terms of the quantitative contributions by different contributing bonding mechanisms.

In this paper, direct Cu-Al₂O₃ bonding was carried out by DC magnetron sputtering without any adhesion layer. Effort has been made to improve the adherence of Cu thin films on polycrystalline Al₂O₃ with different surface roughness as listed in Table 1. According to the ASTM standard D907-70 [11], adhesion is a state of affairs when there is a valence force or mechanical interaction or both the actions taking place to hold the surfaces together. In other definitions, adhesion can be classified into four main categories including interfacial bonding, inter-diffusion bonding, physical anchoring and intermediate layer adhesion [12]. Joint created between Cu thin films and the Al₂O₃ substrate might be not only due to surface adsorption, but also the cumulative effect from other bonding mechanisms. Factors such as surface roughness, porosity, and surface topography will affect the interfacial joining. In order to have a better understanding of a bonded system, it is crucial to examine the bonding mechanisms and quantify their contributions for adhesion improvement. There have been numerous publications dealing with adhesion between heterogeneous material systems such as ceramics and metals. For example, Pazo et al. studied reactions between Ti-based implant alloys and bioactive silica-based coatings in an effort to enhance the adhesion [13]. Chatain's group has extensively studied the wetting behavior of liquid metals and metal alloys on ceramic substrates [14, 15]. Scheu et al. studied the effect of processing conditions and substrate cleaning procedures on the structure, chemistry and bonding between an epitaxial Cu and a single crystal alumina interface by transmission electron microscope [16]. Tanaka et al. used first principles calculation to understand the atomic structures at the interface between Cu and the (0001) facet of alumina [17]. All these efforts represent excellent effort to the qualitative understanding of the wetting / bonding mechanisms in an effort to improve metal /

ceramic bonding. However, attempt to quantitatively assess the contribution from individual factors has been rare or none-existent.

In the current work, the interfacial adhesion was quantified by film adhesion strength measured using a tensile test. A scanning electron microscope (SEM) was used to examine the surface morphology before bonding and after bond break. The interaction between the Cu thin film and the substrate has been investigated by X-ray photoelectron spectroscopy (XPS). Through a series of comparative analyses, the film bonding mechanisms were studied qualitatively and quantitatively whenever possible.

2. Materials and Methods

2.1 Sample Preparation

Polycrystalline Al₂O₃ substrates (Purity of 96 %) with a diameter of 4 inches (~102 mm) and 0.6 mm thickness were purchased from Semiconductor Wafer, Inc. Before film deposition, substrates were diced into the dimensions of 3.0 mm × 3.0 mm × 0.6 mm using a DISCO DFD 6361 dicing saw at the speed of 1.0 mm/s. The sample cutting step was done prior to the deposition in order to prevent film cracking or film delamination. The substrates were subsequently solvent cleaned using acetone and isopropyl alcohol for 10 min each with the aid of ultrasonic agitation. The substrates were then dried in the oven for 3 min at 70 °C.

Cu thin films were coated onto the Al₂O₃ substrates by DC magnetron sputtering using a PRO Line PVD 75 (Kurt J. Lesker Company) sputter. At the beginning of the process, the chamber was

pumped to a vacuum level below 6.66×10^{-3} Pa. With the desired background pressure, the target surface was first cleaned by argon plasma at 50 W for 5 min with the shutter closed for the following purposes: (i) Removal of contaminants, (ii) Cleaning up the oxidized surface, (iii) Establishing an equilibrium state for the system with sufficient time. The deposition process was conducted at a working pressure of 2.00 Pa and a DC power at 300 W. Cu sputter target is 99.99% in purity, and the diameter and the thickness are 3 inch and 0.125 inch respectively. The substrate was mounted face down, and 10 degree off axis with respect to the target. The distance for substrate-to-target was maintained at 20.0 cm. Rotation of the substrate holder was kept at 20 rpm during deposition for better film uniformity. The substrate temperature was monitored by thermocouples mounted on the back of the substrate holder. Throughout this work, there was no heating applied during the film deposition unless specifically mentioned. The substrate temperature increase due to the plasma bombardment was no more than 5 °C. The deposition rate of the Cu thin film under above conditions was found to be 0.3 nm/s. In this study, we used 50 min deposition time, leading to 900 nm in film thickness.

After the Cu film was deposited, a post annealing step was performed directly inside the sputtering chamber under vacuum conditions to prevent oxidation. Two annealing temperatures (100 °C and 300 °C) were applied. The specimens were heated from ambient temperature to the targeted temperatures at a heating rate of 10 °C/min. After the peak temperature was reached, the specimens were held at the temperature for 30 min before the power was cut off. After cooling down to room temperature, the specimens were removed from the chamber. The cooling rate was approximately 1 C° / min.

A comparative study was also conducted using monocrystalline Al₂O₃ substrates (Latech Scientific Supply Pte Ltd) with a surface roughness (root mean square, *rms*) less than 0.5 nm. The purchased monocrystalline substrate in the orientation of (110) has similar surface energy to polycrystalline Al₂O₃ substrate. The cleaning step and the deposition parameters remained the same for both monocrystalline and polycrystalline Al₂O₃ substrates.

2.2 *Materials Characterization and Adhesion Measurement*

For the surface analysis, atomic force microscopy (AFM, DI-3100, Bruker Corporation) was used to measure the surface topography of the substrate in a scan area of 20 × 20 μm. The number of sampling points was 512 along each line. Tapping mode was used with a frequency of 285 kHz. The probe (Arrow NCR-50) is made of silicon with Al coated on the detector side of the cantilever. The tip of the AFM has a radius around 10 - 15 nm. The true contact area of a substrate was calculated using a MATLAB program based on the information of the point coordinates extracted from the AFM measurement. The calculated area was found to be very close to the one generated by the AFM machine itself.

Scanning electron microscopy JEOL JSM 6360 with back scattering imaging was used to analyze the separated surfaces after the tensile test from both the Cu and Al₂O₃ sides. The operation voltage was 15 kV. The results were used to interpret the failure site in the adhesion test.

The sample cross-sectioning was carried out in a dual beam focused ion beam (FIB) built-in with in-lens SEM (FEI Nova Nanolab DualBeam™ 600i). A trench was milled down from the sample

surface to cover the film and the substrate. Prior to the FIB cutting, a layer of Pt was deposited to protect region of interest using Ga ion beam under the voltage of 30kV, and beam current of 0.28 nA. The Pt film was 1 μm in thickness, 12 μm in length, and 1 μm in width. The first step of FIB cutting, the rough cutting, was done by Ga ion under the voltage of 30 kV, and current of 9.3 nA. The cut dimensions were 15 μm (length) \times 20 μm (width) \times 10 μm (depth). After that, a fine polishing was carried out using Ga Ion under voltage of 30 kV and current of 0.92 nA. Observation of the cross sections under the attached SEM was carried out on a tilted angle at 52° under scanning voltage of 5 kV. The film thickness was measured under the cross sections and used to calibrate the deposition rate.

Investigation on the chemical state was carried out by a Kratos Axis Ultra X-ray photoelectron spectroscopy (XPS) system integrated with depth profiling analysis. The sputtering ion beam species was mono Al, and the operating current and voltage were 10 mA and 15 kV, respectively. Calibration of the binding energies was done by locating the C (1s) peak at 284.8 eV as internal reference. Spectra analysis and curve fitting for each element were performed using Casa XPS processing software using the Shirley fitting format.

The contact angle was measured using sessile drop method in a Dataphysics OCA 20 Contact angle instrument. The apparent surface energy of different alumina substrates was measured using three different liquids: distilled water, ethylene glycol and diethylene glycol with known surface energy. The surface energy of the samples was then calculated using the Owens, Wendt, Rabel and Kaelble (OWRK) method [18-20].

The residual stress of the coated film was measured using the X-ray diffraction (XRD) $\sin^2\Psi$ method. The measurement was performed using a Bruker D8 Discover XRD system with Cu $K\alpha_1$ radiation ($\lambda = 1.54 \text{ \AA}$). The voltage was set at 40 kV while the current was fixed at 40 mA during the experiment. The residual stress in a polycrystalline film was computed from the LEPTOS 7.03 software.

The debonding test was performed using an Instron tester 5567 under tensile mode. Typically for quantitative measurement of the adhesion strength, either a shear test or tensile pull tests are performed. In our case, since the Cu film is very thin, pull test was chosen. After the deposition step, the specimen was attached to the test fixture using super glue (Selleys Supa Glue, Australia). The adhesive used is a one-part epoxy glue in liquid form, and is curable under ambient condition. The joined samples were left for at least 12 hours. They were then sent for adhesion test under ambient condition with a load cell capacity of 500 N. The testing speed was fixed at 10.0 $\mu\text{m/s}$. The adhesion strength was calculated from the average value of 10 pieces of tested specimens.

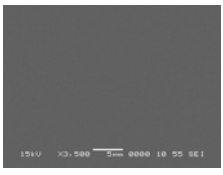
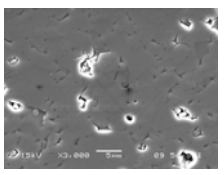
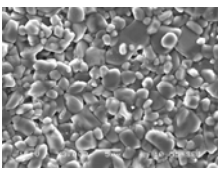
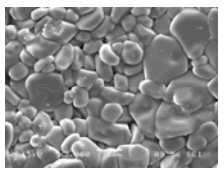
3. Result and Discussion

3.1 Adhesion Strength of Substrates with Different Roughness

As shown in Table 1, polycrystalline Al_2O_3 substrates with different surface roughness (root mean square, *rms*) are grouped in S1 (10 – 150 nm), S2 (200 – 350 nm) and S3 (350 – 500 nm). Substrates from group S1 have been polished through a chemical-mechanical polishing process. Substrates from groups S2 and S3 are the unpolished samples in their as-received state. Top views of the

substrates were shown in the SEM micrographs in Table 1. For polycrystalline Al₂O₃, pores are clearly revealed on the substrate surface and the density of surface porosity increases from S1 to S3. Results are compared with the monocrystalline Al₂O₃ substrate which has a very smooth surface morphology (*rms* < 0.5 nm) and very low surface porosity.

Table 1: Surface analysis of Al₂O₃ substrates with different roughness and interface adhesion of Cu films on these Al₂O₃ substrates

Properties	Monocrystalline Al ₂ O ₃	Polycrystalline Al ₂ O ₃		
		S1	S2	S3
<i>rms</i> (nm)	< 0.5	10 - 150	200 - 350	350 - 500
SEM image				
Adhesion strength (MPa)	5.9 ± 1.5	6.1 ± 1.7	7.7 ± 4.6	8.5 ± 3.2
Apparent surface energy (mJ/m ²)	46.6	51.7	63.3	66.1
True contact area (μm ² , scan area: 20 μm × 20 μm)	400.0	407.5	446.8	486.6
Effective adhesion strength (MPa)	5.9 ± 1.5	6.0 ± 1.6	6.9 ± 4.1	7.0 ± 2.6
Bonding mechanism	Adsorption	Adsorption + Mechanical locking	Adsorption + Mechanical locking	Adsorption + Mechanical locking
Diffusion bonding	No	No	No	No
% enhancement by mechanical interlocking	0	1.7	16.9	18.6

A statistical t-test was done to test the significance in the difference in the mean adhesion strength among different groups in Table 1. At 95% confidence level, there is no significant difference in the mean strength between the monocrystalline and the smooth polycrystalline (S1) groups, indicating negligible effect of the crystalline orientation on the adhesion strength. Comparing S1 and S2 groups, again the two groups are not statistically different at 95% confidence level. However, when comparing S1 and S3 groups, the difference is significant. The same can be said between the monocrystalline group and the S3 group. From the most flat monocrystalline sample (*rms* ~5 nm) to the most rough group S3 (*rms* 350 – 500 nm), an adhesion improvement of 44 % by increasing the substrate surface roughness is visible and statistically significant. In addition, the increase of measured (apparent) surface energy from 46.6 mJ/m² to 66.1 mJ/m² also indicates a better wetting performance of the rough substrate. According to Wenzel's equation (eq. 1), the wetting behavior of a material will be amplified by the surface roughness. The hydrophobicity or hydrophilicity of a material will be enhanced by increasing the surface roughness [21].

$$\cos \theta_m = r \cos \theta_Y \quad (\text{eq. 1})$$

where *r* is the roughness ratio defined as the ratio of true area of the solid surface to the apparent area for actual and projected area of the solid surface, θ_m and θ_Y are the apparent contact angle and Young's contact angle, respectively.

3.2 Correlation between surface roughness and effective area (true contact area)

The effective area of the substrates was calculated using a MATLAB program using the height information at discretized locations measured by AFM. Fig. 1 shows the AFM scan of the surface

profile of a polycrystalline alumina substrate. The true contact area between the film and the substrate is greater than the nominal area because of the surface asperity. Accordingly, effective adhesion strength was calculated, as shown in Table 1, by dividing the force at bond break with the true contact area.

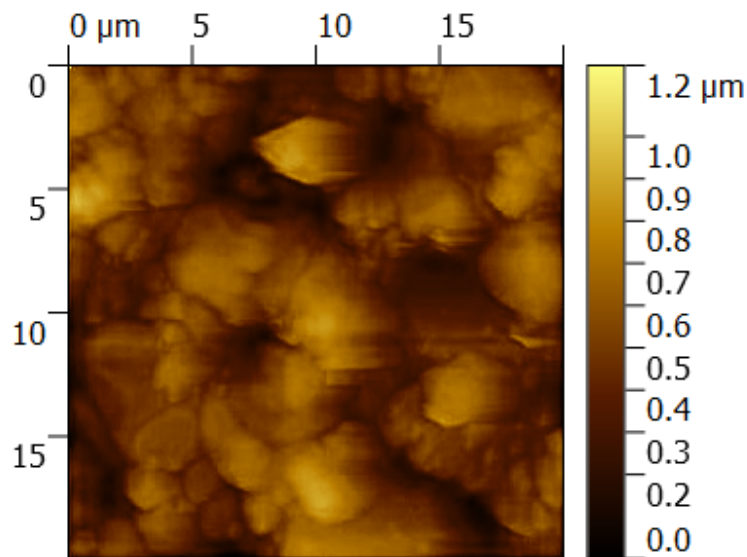


Figure 1: AFM surface profile of a polycrystalline Al_2O_3 substrate.

The relationship of surface roughness to the effective area of a substrate, as indicated in Table 1, shows increased effective area as the roughness increases. This means that the interface contact area is enlarged by the uneven surface structure of the polycrystalline Al_2O_3 substrates. In addition to the rough surface, the surface porosity may have an impact on the $\text{Cu-Al}_2\text{O}_3$ adhesion too. Besides adsorption bonding on the top surface, there is a possibility that the sputtered atoms move down to the porous sites and are locked tightly inside the concaved regions. The monocrystalline Al_2O_3 substrate has a very flat surface, it shows no pores, voids or valley formation on the surface. During the deposition process, it is impossible for mechanical anchoring to take place. We believe

that surface adsorption is the only contributing bonding mechanism in the Cu-monocrystalline Al_2O_3 bonded system.

To observe the film / substrate interface under the SEM, cross-sectioned samples were prepared by either bending or the FIB milling. Fig. 2 shows a fractured cross section by bending, the intimate contact between the Cu film and the Al_2O_3 substrate was observed. The same has occurred for other polycrystalline substrates with different surface roughness. The entire coverage of sputtered Cu films on the polycrystalline Al_2O_3 with irregular surface structure is shown in Fig. 3 (prepared by FIB milling). Throughout the deposition process, ions and/or atoms inside the sputtering chamber are moving ballistically from target to substrate by momentum transfer. The energetic Cu atoms move randomly on the substrate surface or ram into the concave regions before their final settlement. This leads to much improved Cu film adhesion with rough polycrystalline Al_2O_3 which has a higher effective bonding area.

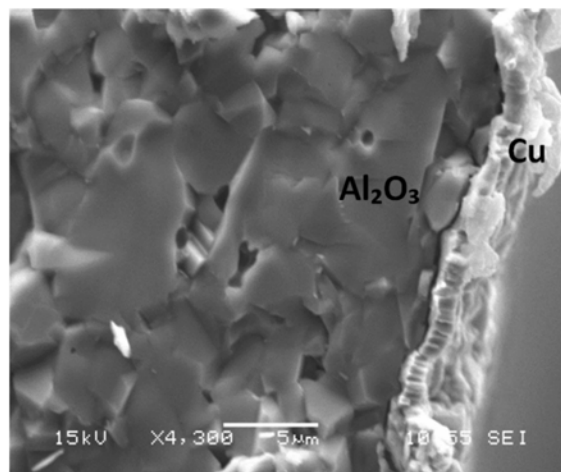


Figure 2: SEM side view image of Cu- Al_2O_3 bonding system with polycrystalline substrate from group S2. The scale bar is 5 μm .

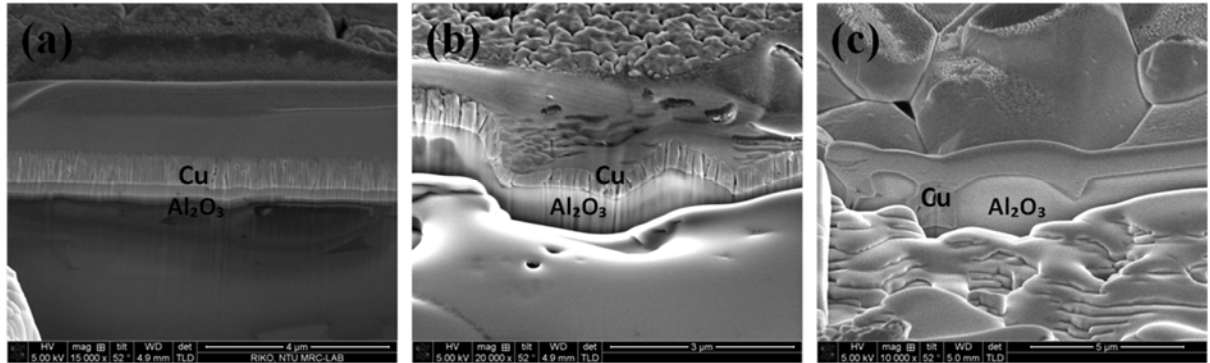


Figure 3: FIB-SEM cross sectional images of Cu-Al₂O₃ bonding using polycrystalline substrates from group (a) S1, scale bar 4 μm; (b) S2, scale bar 3 μm; and (c) S3, scale bar 5 μm.

The reported effective adhesion strength in Table 1 provides an approximation of the contribution to the adhesion enhancement by the mechanical interlocking mechanism. If we use the effective adhesion strength of the monocrystalline sample as the baseline assuming the only contributing mechanism is surface adsorption, contribution from mechanical interlocking will then be differentiated. A detailed discussion will be given in the next two sections.

3.3 Surface Adsorption

As mentioned above, the monocrystalline Al₂O₃ substrate with a very flat surface was used as a baseline to quantify the contribution of various bonding mechanisms. From the SEM inspection in Fig. 4, a clean separation between the Cu thin film and the monocrystalline Al₂O₃ was observed. The very flat surface of the substrate shows no possibility for physical locking bonding to take place. There was indeed no Cu residue on the substrate side after separation. From Fig. 4(b), the grain structure of the Cu thin film is clearly revealed. The smooth surface structure shows no failure such as cracking or buckling in the Cu film itself after the adhesion test.

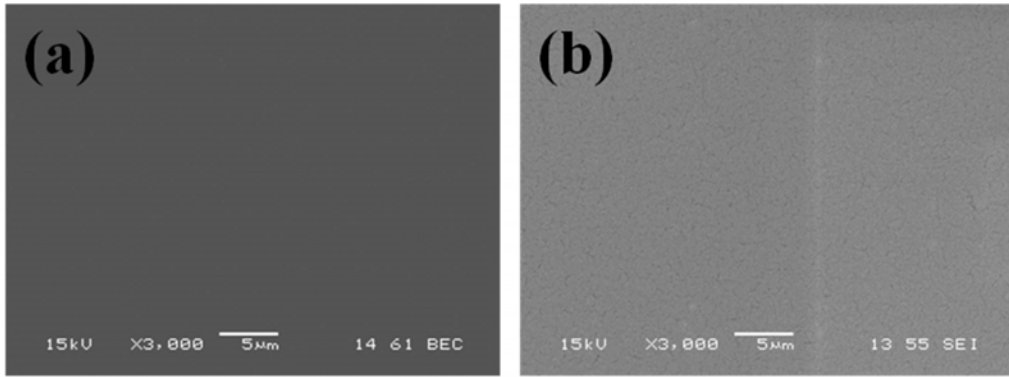


Figure 4: SEM images of separated Cu-monocrystalline Al_2O_3 bonding (a) monocrystalline Al_2O_3 substrate side and (b) copper side.

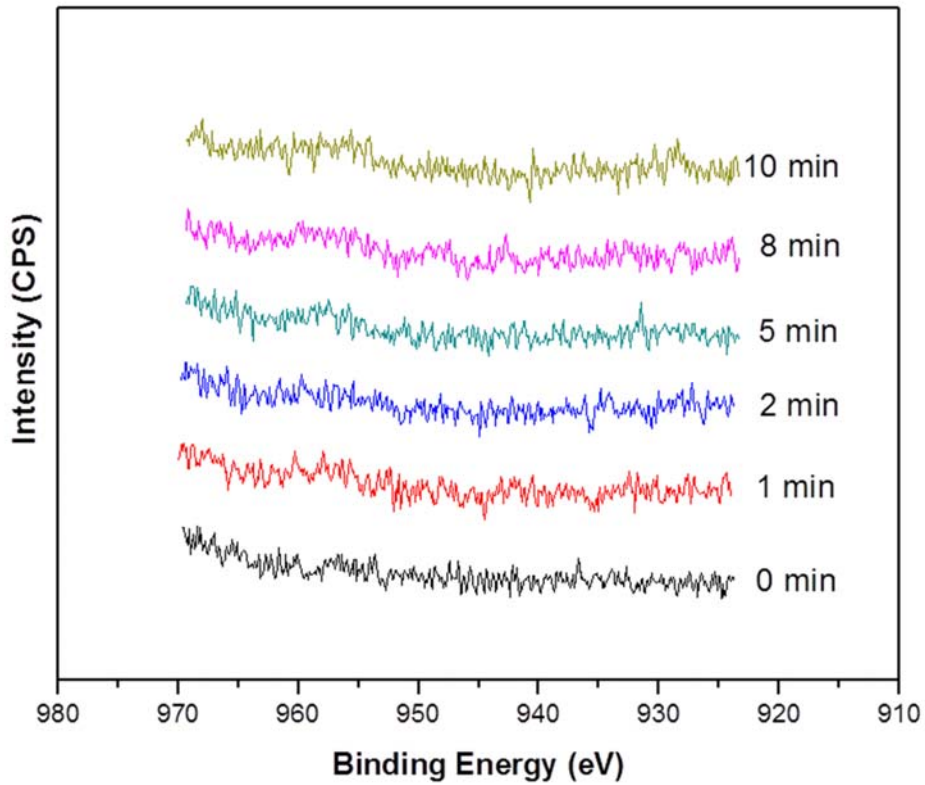


Figure 5: XPS spectra with depth profiling analysis on monocrystalline Al_2O_3 substrate after tensile test. The Ar plasma bombardment time is indicated in the graph.

To further verify this claim, the surface after tensile test was also inspected using XPS combined with depth profiling by argon plasma etching for 0, 1, 2, 5, 8 and 10 min. The purpose was to

examine a possible interaction between the Cu film and the Al₂O₃ substrate. From the XPS spectra analysis with binding energy in the range of 923 to 970 eV in Fig. 5, the Cu 2p peak with an estimated binding energy range from 925 to 960 eV was not detected in the XPS spectra, indicating that there is no residual Cu on this extremely flat substrate surface. This observation supports our early SEM observation that the Cu thin film has been completely detached from the monocrystalline Al₂O₃ substrate after the adhesion test. In addition, it also confirms that there is no chemical reaction between Cu and Al₂O₃. Therefore, physical surface adsorption is suggested to be the only bonding mechanism for Cu-monocrystalline Al₂O₃ bonding which is responsible for the observed low adhesion strength.

3.4 *Mechanical Interlocking*

As discussed above, besides surface adsorption, mechanical interlocking and diffusion bonding mechanisms might exist for rough and polycrystalline substrates. For Cu-polycrystalline Al₂O₃ bonding in group S1, the substrates have a surface roughness (*rms*) in the range of 10 – 150 nm. Fig. 6 shows the SEM images of separated surfaces of Cu and polycrystalline Al₂O₃. There were some Cu residues on the substrate side after separation (Fig. 6 (a)). It is suggested the Cu film has locked mechanically and condensing vapor has been trapped inside the pores during deposition. On the Cu side as shown in Fig. 6 (b), the cracking lines and broken sites are suggestive of a higher separation force to pull the Cu film away from polycrystalline Al₂O₃ as compared with a monocrystalline substrate. This is primarily due to mechanical locking.

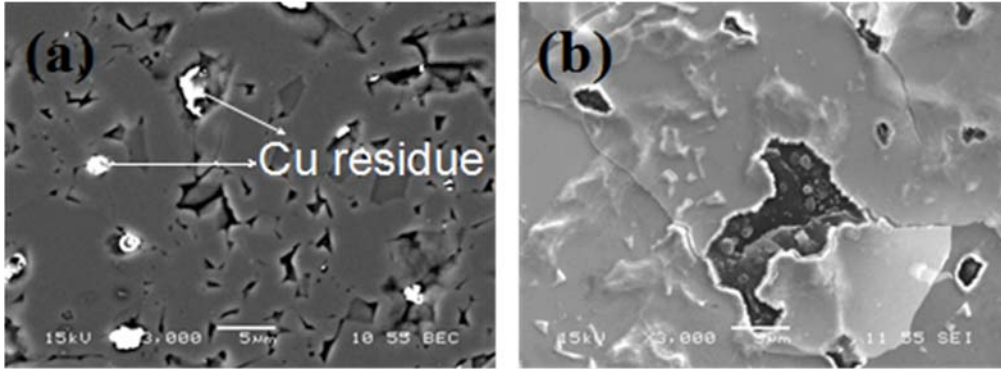


Figure 6: SEM images of separated Cu-polycrystalline Al₂O₃ bonding (a) polycrystalline Al₂O₃ substrate side and (b) copper side. The scale bars in both images are 5 μm.

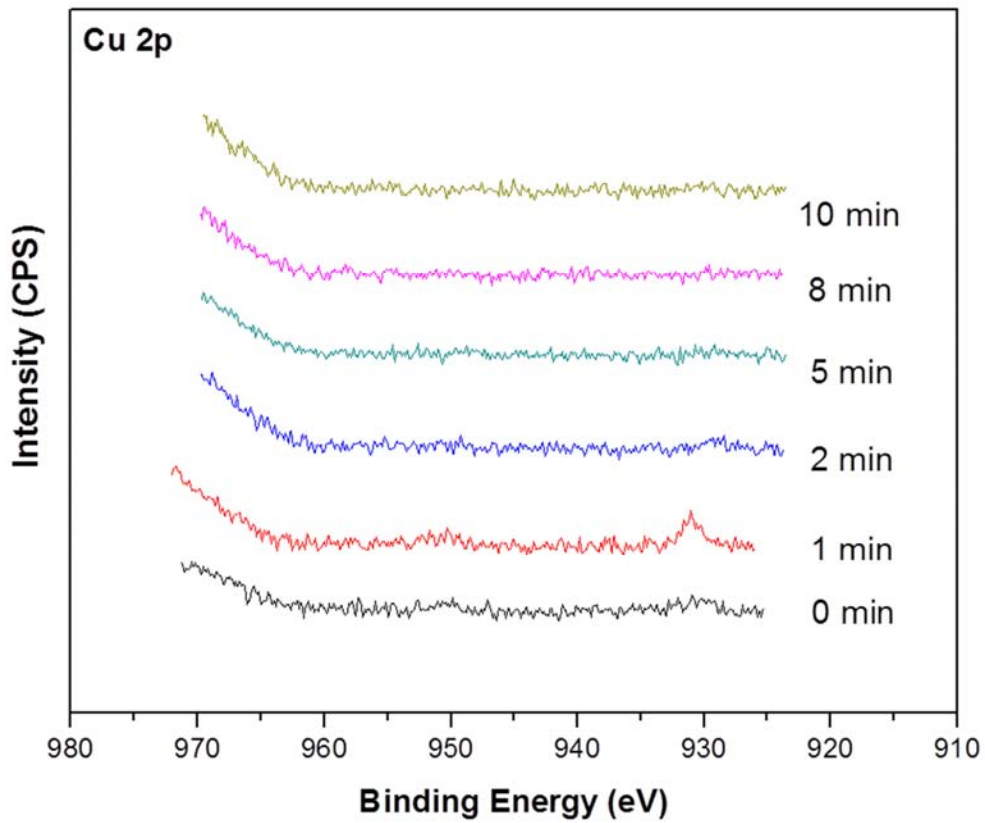


Figure 7: Cu 2p XPS spectra with depth profiling analysis on polycrystalline Al₂O₃ substrate after tensile test

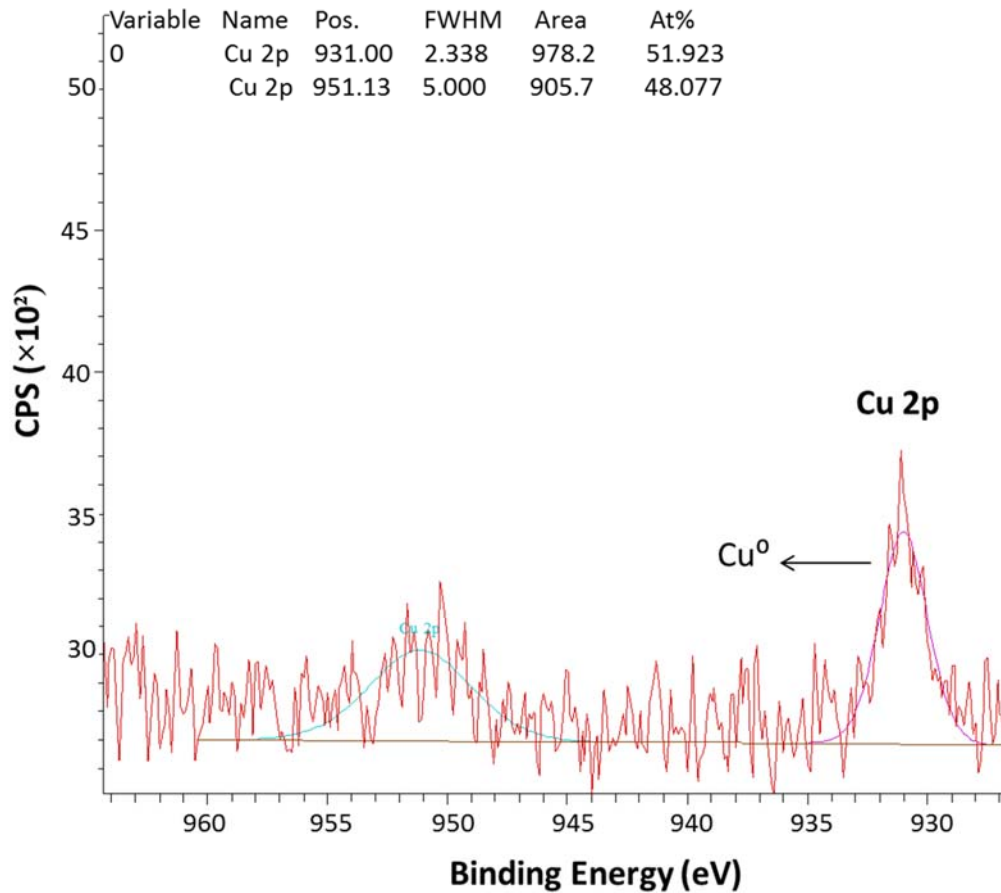


Figure 8: Cu 2p XPS narrow spectrum on polycrystalline Al₂O₃ substrate after 1 min of depth profiling

For Cu-polycrystalline Al₂O₃ bonding, a Cu 2p peak was observed on the substrate surface after 1 min of Ar plasma bombardment of the surface as presented in Fig. 7. However, elemental Cu was not detected in plasma etching times beyond 1 min. On the topmost layer of the substrate (0 min), the Cu film has been completely pulled away from the substrate surface. The results seem to indicate that there was only a small amount of Cu at the sub- but very close to the top surface. With the Cu 2p XPS narrow spectrum analysis in Fig. 8, the obtained binding energies were caused by the splitting of spin orbital for Cu 2p 3/2 (931.0 eV) and Cu 2p 1/2 (951.2 eV) core level

transition respectively. The Cu 2p spectrum was well fit by single component which attributed to the Cu⁰ element [22], and there was no indication of chemical bonding between Cu and Al₂O₃. In addition, oxidized Cu is not detected.

Therefore in Cu-polycrystalline Al₂O₃ bonding, we believe the interfacial adhesion is composed of physical adsorption and mechanical interlocking. Obviously mechanical locking is strongly affected by the surface roughness [23, 24] and the pore density of the substrate. The uneven surface structure of Al₂O₃ has contributed to the increase of adhesion strength for Cu-Al₂O₃ bonding. It is physically straight forward to understand that rough surface is easier to trap sputtered atoms than smooth surface. The porous region increases the chance of atoms settlement which leads to mechanical interlocking.

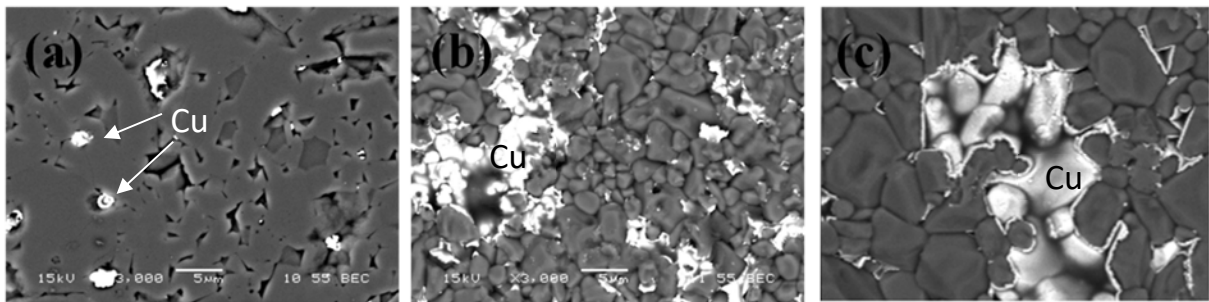


Figure 9: SEM micrographs of substrate surface after the tensile test by using polycrystalline Al₂O₃ with different surface roughness (a) group S1 (b) group S2 and (c) group S3. The scale bars are 5 μm in all images.

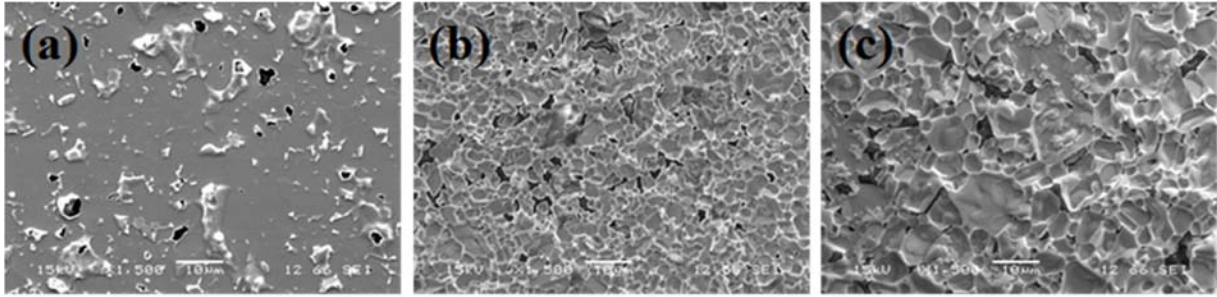


Figure 10: SEM micrographs of the Cu film after the tensile test by using polycrystalline Al₂O₃ with different surface roughness (a) group S1 (b) group S2 and (c) group S3. The scale bars are 10 μm in all images.

The separated surfaces viewed from Cu and polycrystalline Al₂O₃ sides are presented in Fig. 9 and Fig. 10, respectively. The amount of Cu residue has increased with the substrate surface roughness from S1 (10 – 150 nm) to S3 (350 – 500 nm), and these residues preferably stayed around the porous regions (Fig. 9). From the SEM images in Fig. 10, similar surface features on the detached Cu films are observed. This proves that the Cu film is deposited by closely following the surface profile of the substrate. The observed broken sites on the Cu thin film suggest a strong mechanical locking effect between the Cu thin film and the polycrystalline Al₂O₃ substrate. The observation indicates that, besides atoms adsorption on the surface, sputtered Cu atoms with high mobility have sufficient energy to travel into the deeper region of the substrate sub-surface via pores and voids.

The preceding investigation is based upon the assumption that the true contact area of the monocrystalline Al₂O₃ substrate is 400 μm² due to its extremely low surface roughness (< 0.5 nm). With the baseline study from Cu-monocrystalline Al₂O₃ bonding (indicated by the red dotted line in Fig. 11), Table 1 lists the effective adhesion strength, defined as the bond breaking load per unit

actual surface area based on the AFM measurement. Based on the effective adhesion strength data, the contribution of mechanical interlocking accounts for 1.7 % (group S1) to 18.6 % (group S3) of the increased adhesion strength.

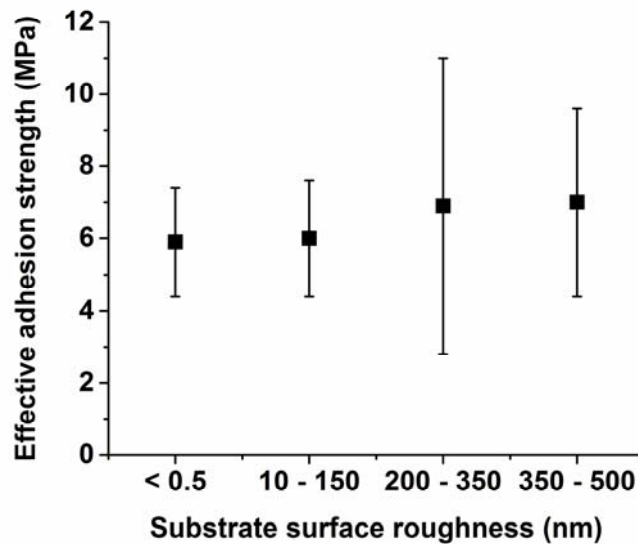


Figure 11: Impact of substrate surface roughness on the effective adhesion and the bonding mechanisms between Cu thin film and Al₂O₃ substrates

3.5 Diffusion Bonding

At the as-deposited state, diffusion of Cu atoms into the lattice or grain boundaries of the substrate is quite unlikely due to the low deposition temperature and short duration. Following the previous discussion, surface adsorption and mechanical interlocking are the only contributing factors to the observed adhesion. In this section, the possibility of diffusion bonding is analyzed by applying in-situ post deposition annealing at 100 °C and 300 °C respectively for 30 min under argon gas atmosphere (pressure = 2 MPa). Monocrystalline and polycrystalline S1 substrates were used for this study.

Post annealing is commonly used to alleviate the internal stress induced during the deposition to prevent interface delamination [25]. However, from Fig. 12, post annealing has weakened the interfacial bonding between Cu and the monocrystalline Al₂O₃ substrate. The adhesion strength dropped from 5.9 ± 1.5 MPa (room temperature) to 3.2 ± 1.3 MPa after the 300 °C annealing. The Cu film stress was in the compressive state, the magnitude has increased from -111.8 MPa (as deposited) to -147.6 MPa after 300 °C annealing for 30 min. On the other hand, the Cu film stress for the polycrystalline substrate was in tension and it decreased from 116.7 MPa to 53.3 MPa after annealing. The exact reason for this opposite trend requires further investigation, and it is suspected the presence (or absence) of grain boundaries and surface pores, being regions able to accommodate diffused Cu atoms, might be the reason for the difference. The lack of such surface features in monocrystalline Al₂O₃ substrate might have prevented the migration of Cu atoms into the porous structures, preventing stress relief.

Eisenmenger-Sittner et al. [26] found that Cu film could de-wet from carbon (graphite) substrate when heated at 800 °C. The de-wetting has led to decreased adhesion between the Cu film and the substrate. This factor is unlikely to be operative in the current study because the highest heating temperature was only 300 °C. Based on Fig. 10, the Cu surfaces clearly replicate the alumina grain feature, indicating that there is no de-wetting between the Cu and the alumina substrate.

The mean adhesion strength with polycrystalline Al₂O₃ bonding (group S1) improved by 18% after post annealing at 300 °C for 30 min. There are two potential factors behind the improvement. The first one could be the reduction of the film stress which has reduced the stored elastic energy in

the film. Such a reduction helps the enhancement of film adhesion. The second factor could be Cu diffusion deeper into the pores and voids, which will be analysed further later.

SEM inspection was carried out on the separated surfaces as shown in Fig. 13 for Cu-monocrystalline Al₂O₃ bonding. From Fig. 13(a), cracking lines were evidently exposed on the monocrystalline Al₂O₃ substrate. Cu film cracking was observed in Fig. 13 (b). The substrate surface cracking might be caused by the tensile stress imposed by the Cu film although the exact magnitude of such stress is difficult to estimate.

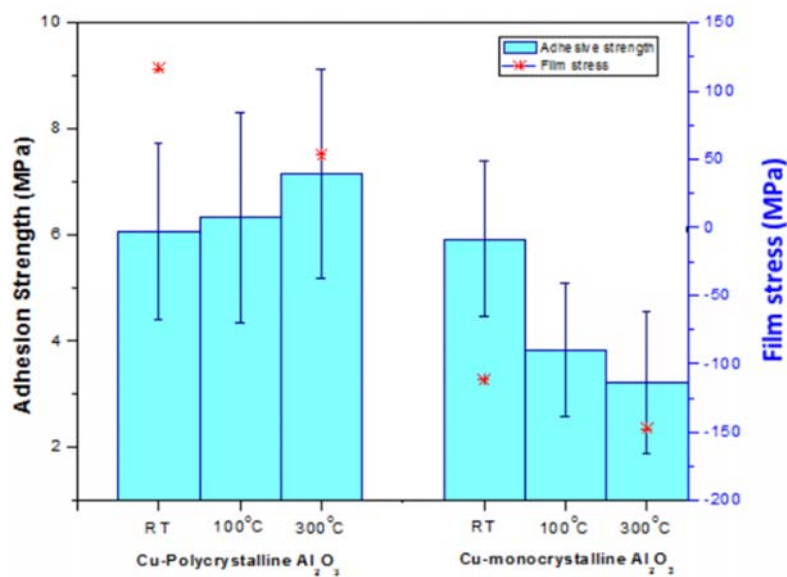


Figure 12: Effect of in-situ post annealing to the Cu-Al₂O₃ adhesion strength and film stress.

For Cu-polycrystalline Al₂O₃ bonding, the separated surfaces of the annealed sample show similar features (Fig. 14) as the ones without post-annealing. A high percentage of the substrate surface has been occupied by Cu residues under high temperature heating as indicated in Fig. 14 (a). This is in agreement with the observed adhesion improvement.

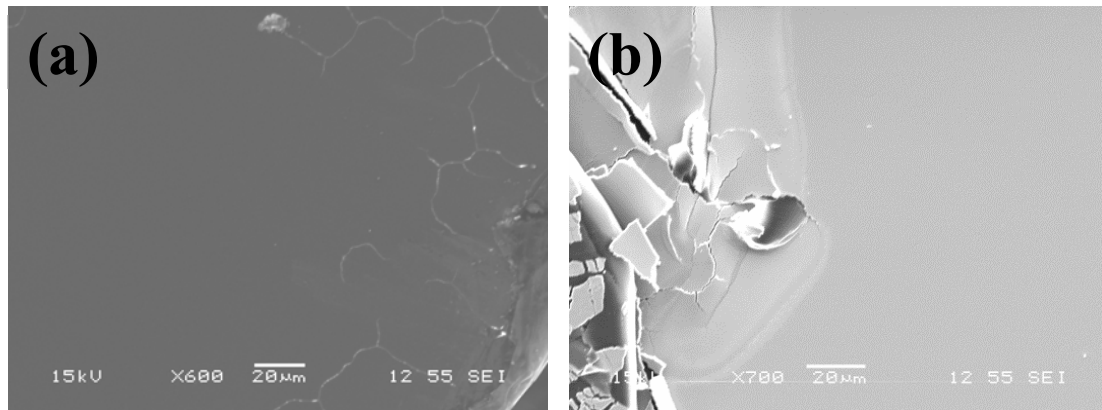


Figure 13: SEM images of separated Cu-monocrystalline Al₂O₃ bonding after post annealing at 300 °C for 30 min (a) monocrystalline Al₂O₃ substrate side and (b) copper side.

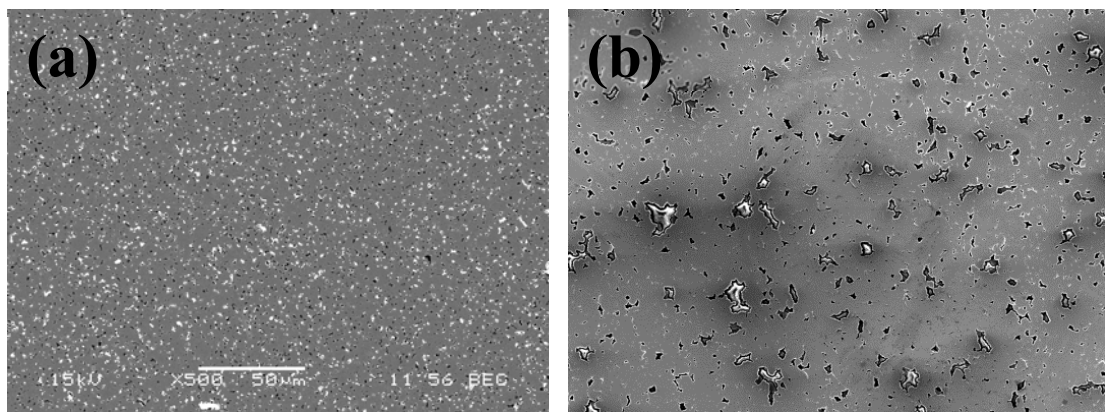


Figure 14: SEM images of separated Cu-polycrystalline Al₂O₃ bonding after post annealing at 300 °C for 30 min (a) polycrystalline Al₂O₃ substrate side and (b) copper side. Same scale bar is applied for the images.

To further investigate the distribution of Cu in the substrate, XPS analysis integrated with depth profiling was conducted on the substrate after film separation. Plasma etching for up to 10 min was carried out on the substrates annealed at 300 °C for 30 min (Fig. 15). On the monocrystalline Al₂O₃ surface, no indication of elemental Cu was observed within the binding energy range of 923 eV to 970 eV (Fig. 15 (a)). The clean separation at the interface confirms the absence of physical locking or diffusion bonding mechanisms in the monocrystalline substrate. However, Cu 2p peaks

were detected on the polycrystalline Al₂O₃ substrate after 2 and 10 min Ar plasma etching. Based on reported Cu (Cu⁰, Cu⁺ and Cu²⁺) binding energies [27], the Cu 2p 3/2 orbital in Fig. 16 was only well fitted by Cu⁰ with a binding energy of 932.45 eV. Formation of cupric oxide (CuO) and cuprous oxide (Cu₂O) was not detected. It is also confirmed by the O 1s XPS narrow spectrum that no chemical reaction has taken place between Cu and oxygen. The Cu 2p peaks were not visible for surface scans due to the very low signal-to-noise ratio. The presence of Cu atoms deeper inside the substrate is evident when compared with the XPS depth profile of an untreated sample. We attribute the increase of the adhesion strength of the polycrystalline sample to the diffusion of Cu into deeper subsurface regions of the substrate, as well as the relief of film stress. The increase of adhesion strength is about 18 % after annealing; however we are not able to distinguish the exact contribution from diffusion mechanism and stress relief. Future investigation is needed to further clarify this point. Based on above analyses, it might be helpful to deposit the Cu films at an elevated temperature to draw the benefit of enhanced diffusion bonding. Nevertheless, this is not within the scope of the current study.

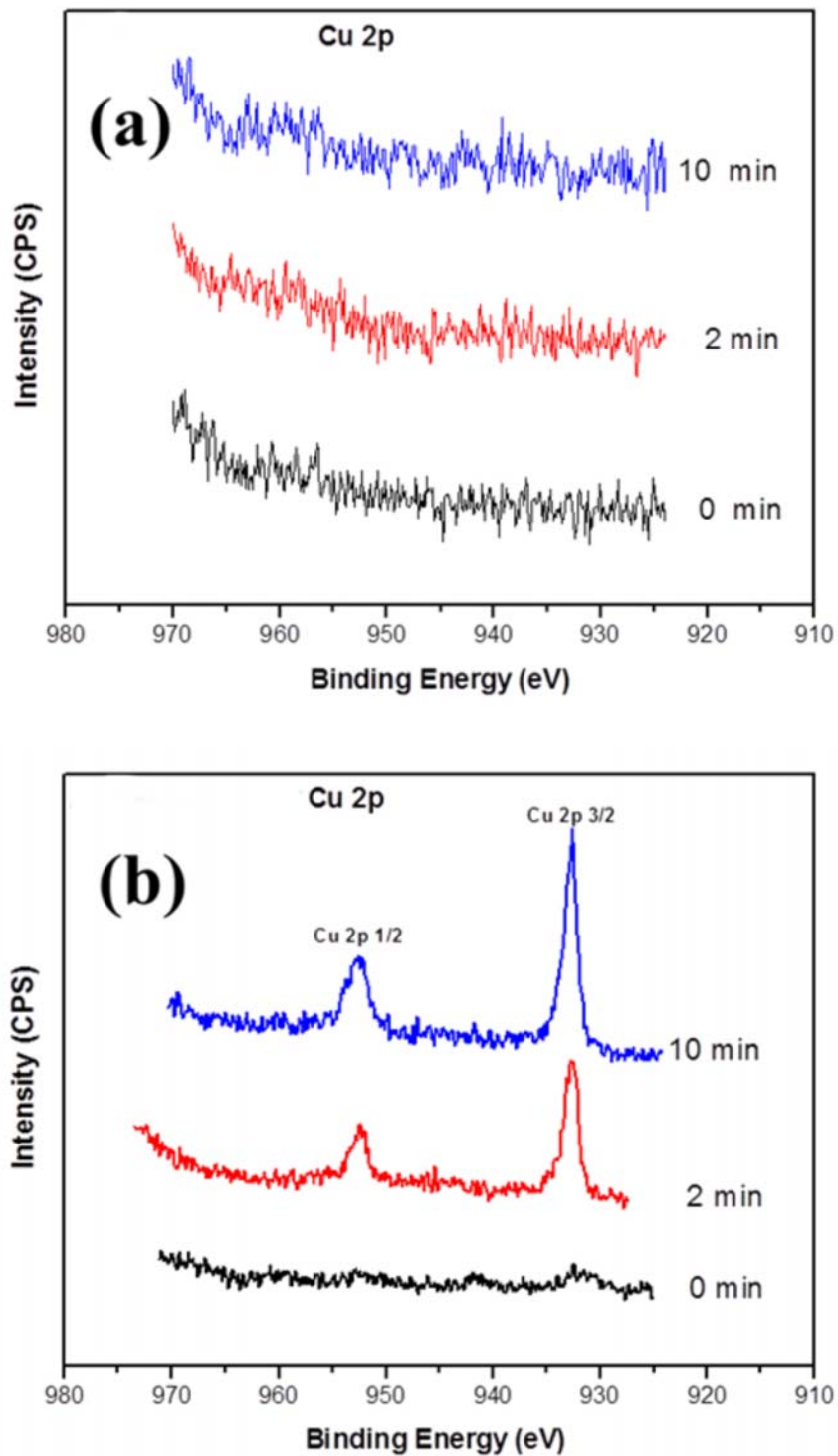


Figure 15: XPS spectra with depth profiling analysis on post-annealed (a) monocrystalline Al_2O_3 and (b) polycrystalline Al_2O_3 substrate after the tensile test.

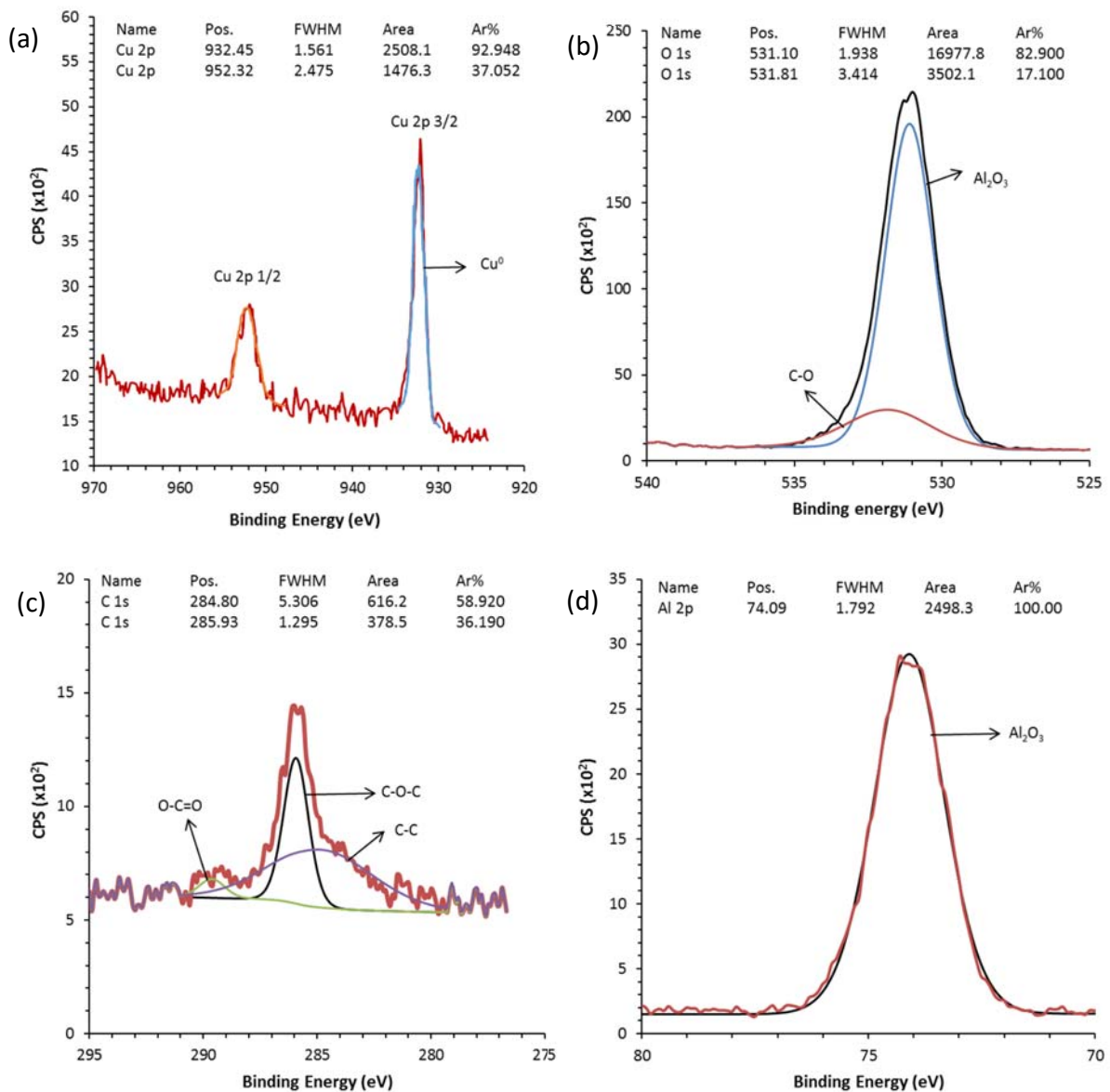


Figure 16: XPS narrow (a) Cu 2p, (b) Al 2p, (c) O 1s and (d) C 1s spectra of post-annealed polychrystalline Al₂O₃ substrate after 10 min depth profiling with Ar⁺.

4. Conclusion

Different types of bonding mechanisms have been studied for their contribution to adhesion between a directly sputtered Cu film and an Al₂O₃ substrate. Surface adsorption provides the main contribution to the observed adhesion strength. A comparison between substrates with very low

roughness and the ones with higher roughness and surface porosity has revealed that mechanical interlocking is a contributing factor behind the observed adhesion strength increase in the latter. Quantitatively, the mechanical interlocking bonding mechanism has contributed up to 18.6 % to the Cu film adhesion to an Al₂O₃ polycrystalline substrate with a surface roughness of 350 - 500 nm. A diffusion bonding mechanism may be operative only with post deposition annealing treatment. Post-deposition annealing at 300 °C has contributed comparably to the improvement in film adhesion as mechanical interlocking does, however at this stage we are not able to quantify a precise number for the contribution of the diffusion bonding mechanism as the film stress has also changed during annealing. XPS analysis confirms that Cu atoms have diffused deeper into the substrate, but there is no chemical reaction between Cu with either the residual oxygen in the chamber or the Al₂O₃ substrate during the annealing treatment.

Acknowledgement

JDL acknowledges the scholarship provided by GLOBALFOUNDRIES Pte Ltd, Singapore. Technical assistance by Dr. Riko I Made, Mr. Daniel A. Bellido Aguilar, and Mr. Bo Zheng is very much appreciated.

References

1. D.M, Aluminum-nitride copper bonding improves MCMs. *Electronic Design*, 1994. 42(4): p. 27.
2. Paik, K.W. and C.A. Neugebauer, Direct bonding of copper to aluminum nitride substrates, Harris Corporation, 1995. US5418002A.
3. Burgess, J.F., C.A. Neugebauer, G. Flanagan, R.E. Moore, The direct bonding of metals to ceramics and application in electronics. *Active and Passive Electronic Components*, 1976(4): p. 233.
4. Djokic, S., R. Lepard, and R. Roy, Electroless/electrolytic methods for the preparation of metallized ceramic substrates, 1995. US5849170A.

5. Ning, X.-S., Y. Lin, R. Peng, H. Zhou, K. Chen, Development of a directly bonded aluminum/alumina power electronic substrate. *Materials Science and Engineering: B*, 2003. 99(1–3): p. 479-482.
6. Entezarian, M. and R.A.L. Drew, Direct bonding of copper to aluminum nitride. *Materials Science and Engineering: A*, 1996. 212(2): p. 206-212.
7. Zhang, G.Q., W.D. Driel, and X.J. Fan, *Mechanics of microelectronics* [electronic resource]. Dordrecht: Springer, 2006. (Solid Mechanics and Its Applications: 141). ISBN: 9781402049354
8. Yoshino, Y., Role of oxygen in bonding copper to alumina. *Journal of the American Ceramic Society*, 1989. 72(8): p. 1322-1327.
9. Zhang, G., J. Zhang, P. Yi, D. Chai, Joining of Al₂O₃/Al composites by transient liquid phase (TLP) bonding and a novel process of active-transient liquid phase (A-TLP) bonding. *Materials Science & Engineering A*, 2008. 488: p. 146-156.
10. Wielage, B., T. Grund, C. Rupprecht, S. Kuemmei, New method for producing power electronic circuit boards by cold-gas spraying and investigation of adhesion mechanisms. *Surface and Coatings Technology*, 2010. 205(4): p. 1115-1118.
11. ASTM D907-70, in *Definition of terms relating to adhesion*: American Society for Testing and Materials.
12. Chapman, B.N., Thin Film Adhesion. *Journal of Vacuum Science and Technology*, 1974. 11: p. 106-113.
13. Paso, A., E. Saiz, A. P. Tomsia, Silicate Glass Coatings on Ti-based Implants, *Acta Materialia*, 1998, 46(7): p. 2551-2558
14. Ghetta, V., J. Fouletier, D. Chatain, Oxygen Adsorption Isotherms at the Surfaces of Liquid Cu and Au-Cu Alloys and Their Interfaces with Al₂O₃ Detected by Wetting Experiments, *Acta Materialia*, 1996, 44(5): p. 1927-1936
15. Chatain, D, F. Chabert, V. Ghetta, New Experimental Setup for Wettability Characterization under Monitored Oxygen Activity: I, Role of Oxidation State and Defect Concentration on Oxide Wettability by Gold, *Journal of American Ceramics Society*, 1993, 76(6): p. 1568-1576
16. Scheu, C., M. Gao, S. H. Oh, G. Dehm, S. Klein, A. P. Tomsia, M. Rühle, Bonding at copper–alumina interfaces established by different surface treatments: a critical review, *Journal of Materials Science*, 2006, 41: p. 5161-5168
17. Tanaka, S., R. Yang, M. Kohyama, T. Sasaki, K. Matsunaga, Y. IKuhara, First-Principles Characterization of Atomic Structure of Al₂O₃(0001)/Cu Nano-Hetero Interface, *Materials Transactions*, 2004, 45: p. 1973-1977
18. Kaelble, D.H., Dispersion-Polar Surface Tension Properties of Organic Solids. *The Journal of Adhesion*, 1970, 2: p. 66-81.
19. Owens, D., R. Wendt, Estimation of the Surface Free Energy of Polymers. *Journal of Applied Polymer Science*, 1969. 13: p. 1741-1747.
20. Rabel, W., Einige Aspekte der Benetzungstheorie und ihre Anwendung auf die Untersuchung und Veränderung der Oberflächeneigenschaften von Polymeren. *Farbe und Lack*, 1971. 77: p. 997-1005.
21. Wenzel, R.N., Resistance of solid surfaces to wetting by water. *Industrial & Engineering Chemistry*, 1936. 28(8): p. 988-994.

22. Naumkin, Alexander V., A. Kraus-Vass, Stephen W. Gaarenstroom, and Cedric J. Powell, NIST X-ray photoelectron spectroscopy database, NIST Standard Reference Database 20, Version 4.1 2012, U.S. Secretary of Commerce on behalf of the United States of America
23. Lin, Y.S. and H.M. Liu, Enhanced adhesion of plasma-sputtered copper films on polyimide substrates by oxygen glow discharge for microelectronics. *Thin Solid Films*, 2008. 516(8): p. 1773-1780.
24. Yang, C.-H., S.-C. Lee, J.-M. Wu, T.-C. Lin., The properties of copper films deposited on polyimide by nitrogen and oxygen plasma pre-treatment. *Applied Surface Science*, 2005. 252(5): p. 1818-1825.
25. Puchert, M.K., P.Y. Timbrell, and R.N. Lamb, Postdeposition annealing of radio frequency magnetron sputtered ZnO films. *Journal of Vacuum Science & Technology A*, 1996. 14(4): p. 2220-2230.
26. Eisenmenger-Sittner, C., E. Neubauer, C. Schrank, J. Brenner, C. Tomastik, Solid state de-wetting of vapor deposited films on planar and fiber-shaped carbon substrates, *Surface and Coatings Technology*, 2004. 180-181: p. 413-420.
27. Goh, S.W., A.N. Buckley, R.N. Lamb, R.A. Rosenberg, D. Moran, The oxidation states of copper and iron in mineral sulfides, and the oxides formed on initial exposure of chalcopyrite and bornite to air. *Geochimica et Cosmochimica Acta*, 2006. 70(9): p. 2210-2228.